APPROVED FOR PUBLICATION AAEC/TM581

AAEC/TM581

AUSTRALIAN ATOMIC ENERGY COMMISSION
RESEARCH ESTABLISHMENT
LUCAS HEIGHTS

PROMPT NEUTRONS FROM ^{236}U FISSION FRAGMENTS

by

J.W. BOLDEMAN
A.R. de L. MUSGROVE
R.L. WALSH

March 1971

APPROVED FOR PUBLICATION

ISBN 0 642 99408 0

AUSTRALIAN ATOMIC ENERGY COMMISSION

RESEARCH ESTABLISHMENT

LUCAS HEIGHTS

PROMPT NEUTRONS FROM ^{236}U FISSION FRAGMENTS

by

J.W. BOLDEMAN

A.R. de L. MUSGROVE

R.L. WALSH

ABSTRACT

Measurements were made of prompt neutron emission in the thermal neutron fission of ^{235}U. The mean neutron emission per fragment was obtained for particular values of the fragment mass and total kinetic energy. A direct neutron counting method was employed and a comparison made with data from previous experiments of this type.

NOTE: This paper has been submitted to a journal. Further details can be obtained from the authors or the Director of the Research Establishment.

National Library of Australia card number and ISBN 0 642 99408 0

CONTENTS

1. INTRODUCTION

A detailed investigation has been commenced into the energy balance at scission in the fission process. The program will include measurements of neutron emission from individual fission fragments as a function of their mass and charge and of the total fragment kinetic energy for both ternary and binary fission. The paper reports a preliminary measurement of the mean neutron emission per fragment as a function of the fragment mass and total fragment kinetic energy in the thermal neutron fission of ^{235}U.

Two methods have been employed in recent years to obtain data of this type. One method devised by Terrell (1962) involves a comparison of pre-neutron and post-neutron emission mass yield data obtained in double time of flight and double kinetic energy studies. This method is highly satisfactory when the parameters are restricted to fragment mass and total fragment kinetic energy. However, if additional parameters such as the nuclear charge are sought, an alternative method is required because the count rate in these circumstances becomes vanishingly small.

The other method involves the direct counting of the neutrons (- Milton and Fraser 1965, Apalin et al. 1965 and Maslin et al. 1967). This method is possible because at least 85 per cent of the neutrons are emitted from the fragments after they have reached their terminal velocities. The angular distribution in the laboratory system of neutron emission from a particular fragment is therefore strongly peaked in the fragment direction. Consequently a neutron detector geometrically located in the fragment direction will detect, preferentially, neutron emission from that fragment.

The neutron emission versus fragment mass data that have been obtained are important for an understanding of the energy balance at scission. The variation of neutron emission with mass has revealed that this is determined more by the properties of the fragments than by the mass ratio. The details of the variation have shown the influence of shell effects in determining the scission configuration and have been explained in terms of the deformability of the fragments. In fact Terrell (1965) has used the measured variation to obtain the deformation parameters of the neutron rich fission fragment species of nuclei.

The most recently published experiment (Maslin et al. 1967), highlights discrepancies in the measured magnitude of the variation of neutron emission with fragment mass. The present experiment confirms the data of Maslin et al. and provides higher statistical accuracy for some of the secondary relationships.

2. EXPERIMENTAL SYSTEM

The experimental system is shown schematically in Figure 1. A highly collimated beam of thermal neutrons was obtained from the 10 MW reactor HIFAR. The neutrons emerge from the graphite reflector of the reactor and consequently

the fast neutron and epithermal components of the beam are very small (Boldeman et al. 1962). The thermal neutron flux at the experiment was 1.5 x 10^7 n cm^{-2} sec^{-1} and the beam diameter 1.5 cm.

The fragment detectors and ^{235}U target were placed in a high vacuum of approximately 2 x 10^{-8} torr which was maintained with a getter ion pumping system. The neutron beam entered and left the vacuum system via 0.012 cm thick Al windows. The two fission fragment detectors were typical surface barrier diodes made of n type silicon and operated at 90 V reverse bias. Both detectors were collimated to active areas of 3 cm^2. Detector 1 was located approximately 2.5 cm from the ^{235}U target and consequently subtended an angle of $\pm 22^{\circ}$. Detector 2 was mounted on a linear motion feed-through and its position in the vacuum system could be accurately varied externally. This detector was positioned 6.5 cm from the ^{235}U target and defined the maximum divergence from the axis of the detector system of the selected fission fragments ($\pm 8^{\circ}$). The geometrical arrangement used prevents discrimination against fragments emitting high numbers of neutrons. In principle it would have been preferable to have detector 1 define the fragment geometry, but the spatial requirements of such an arrangement reduce the geometrical efficiency of the scintillator tank.

The ^{235}U targets were prepared by electrospraying ^{235}U nitrate in ethanol solution onto gold plated VYNS films. The ^{235}U target, gold layer and VYNS film thicknesses were respectively 30 μg cm^{-2}, 15 μg cm^{-2} and 20 μg cm^{-2}. The ^{235}U target was placed at 45° to the axis of the fragment detectors and the neutron beam.

The neutron detector was a large liquid scintillator tank containing approximately 60 litres of NE 323, a trimethyl benzene scintillator containing a loading of 0.5 per cent by weight gadolinium. The operation of such detectors in fission neutron counting is well known and details may be found in Boldeman and Dalton (1967). The size of the scintillator tank was a compromise between neutron detection efficiency and background count rate in the reactor environment. Two 9618A photomultiplier tubes mounted on the outside of the tank recorded scintillations resulting from neutron capture events in the gadolinium loading of the scintillator. The mean neutron lifetime in the scintillator before capture is 8 μsec. For calibration purposes, a 3 inch diameter tube was placed axially through the tank. A ^{252}Cf spontaneous fission counter could be placed in this tube and the 4π geometry neutron detection efficiency of the scintillator was obtained by comparing the mean neutron count per spontaneous fission of ^{252}Cf with an assumed value of $\bar{\nu}_p$ for this process of 3.782. Under optimum conditions the 4π neutron detection efficiency was found to be 65 per cent. After calibration the axial tube was removed for this experiment.

3. ELECTRONICS

A block diagram of the electronics is shown in Figure 2. Fast logic timing and slow pulse height signals were obtained from each fragment detector. A fast coincidence (τ = 10 nsec) between the fragment detectors gated the 256 channel analogue to digital convertors on the fragment pulse height lines. The double fragment coincidence signal, after a delay of 300 nsec, also initiated the operation of the Multiple Event Analyser (M.E.A.) on the liquid scintillator output. The M.E.A. operated as follows: the fragments' coincidence signal triggered a 15 μsec wide counting gate on the output of the photomultiplier tubes' coincidence unit, during which time neutron pulses from the associated fission event were scaled with random background pulses. The optimum neutron counting gate was 30 μsec for high neutron counting efficiency but the 15 μsec gate was chosen in the reactor environment to optimise neutron to background count rates. In addition the severe background problem made it necessary to operate the scintillator tank at reduced efficiency. The 4π operating efficiency for the entire experiment was approximately 25 per cent. After a duration of 60 μsec, a second 15 μsec gate recorded the background. Background pulses were counted in a separate scaler within the M.E.A. The M.E.A. could store up to 15 counts in the foreground channel and seven counts in the background channel for each fission event. In this way it was originally hoped to obtain information on the distribution of neutron emission for a particular fission fragment. However, the restrictions on the scintillation efficiency enforced by the high background severely reduced the accuracy of the distribution data and the analysis of the data was not extended to obtain this information.

All data were recorded event by event on magnetic tape using an incremental tape recorder. Any particular fission record consisted of three bytes of information. The first two bytes were the digitised outputs from the fragment detectors and the third byte contained the foreground and background data from the scintillator tank.

4. ANALYSIS OF DATA

A total of 2×10^7 fission fragment coincidences were recorded. The preliminary analysis of the data consisted of visual inspection of the fragment pulse height spectra to check electronic drifts and of the scintillator background data to assess constancy of its efficiency. For this purpose raw data were printed out in groups of 100,000 fission events. In practice pulse height drifts (determined by fragment kinetic energy peak positions) were found to be less than 0.1 per cent per 5×10^5 fission events and the variations in the scintillator background rate were less than 2 per cent per 5×10^5 fission events. As a consequence, the data were analysed in groups of 5×10^5 fission events which proved to be a convenient size for computing.

The raw kinetic energy data were used to obtain the pre-neutron emission masses and kinetic energy using the procedures of Schmitt et al. (1965) and Terrell (1962). The method was as follows: A linear calibration of the pulse height scales for each detector was made using the fragment spectra peak positions and experimental data from Milton and Fraser (1962). The approximate pre-neutron emission masses were then obtained from the kinetic energy data using the relationships

$$M_1 = \frac{236\ E_2}{E_1 + E_2} \qquad \ldots(1)$$

$$M_2 = 236 - M_1 \qquad \ldots(2)$$

Post-neutron emission masses were obtained from M_1 and M_2 using the (ν, E_T) data from Maslin (1967). The detector energy scales were recalibrated using the procedure of Schmitt et al. (1965, 1966)

i.e. $$E = (a + a'M)\ x + b + b'M \qquad \ldots(3)$$

where E is the fragment kinetic energy
M is the fragment mass
x is the pulse height
and a, a', b, b' are constants given in Table 1.

Table 1

Calibration Constants

The values P_L and P_H are the observed pulse heights corresponding to the mid points between the 3/4 maximum points in the light and heavy mass groups.

$a = \frac{30.9734}{P_L - P_H}$	$a' = \frac{0.04596}{P_L - P_H}$
$b = 87.8626 - aP_L$	$b' = 0.1345 - a'P_L$

The recalculated post-neutron emission kinetic energies were converted into pre-neutron emission energies using equation 4.

$$E_{Pre} = \frac{E_{Post}}{1 - \frac{\nu}{M}} \qquad \ldots(4)$$

where the ν data as a function of mass and total kinetic energy were obtained as before from Maslin et al. (1967). The entire process was repeated until the pre-neutron emission masses before and after a particular iteration were the same to within 0.1 a.m.u. The output data for each particular fission event consisted of pre-neutron emission masses and total kinetic energy, plus neutron and background data.

To correct the neutron data for scintillator geometry and backscatter from the complementary fragment, the data were sorted into two matrices giving the number of events and the measured mean number of neutrons detected for each value of the mass and total kinetic energy. The mean number of neutrons is obtained from the difference of the mean count in the foreground and background channels of the multiple event counter. The mass groups were 2 a.m.u. wide and the total kinetic energy groups 5 MeV wide. The neutron data were not corrected for dead time losses as this correction was less than 1 per cent. The detector geometry and backscatter correction assumed

1. The excitation energies of the two fragments are correlated, and
2. The detection efficiency of the scintillator is constant with neutron energy.

The correction procedure was as follows. An approximate correction for detector geometry and backscatter was made assuming that all neutrons are emitted from the moving fragments. The data obtained were normalised to $\bar{\nu}_p$ (thermal) ^{235}U = 2.415 (Boldeman and Dalton 1967). This gave an approximate value of the average scintillator efficiency and the variation of ν_T (total neutron emission from both fragments) with fragment mass. Assuming that 15 per cent of the neutrons are emitted isotropically in the laboratory system (Milton and Fraser 1965) the experimentally observed probabilities were adjusted to remove the scission neutron component contributions. The remaining contributions (i.e. from neutrons correlated with the fragment direction) were corrected for detector geometry and backscatter and the variation of $\epsilon\nu_F$ with fragment mass obtained. Here ϵ is the neutron detection efficiency of the scintillator and ν_F the mean number of neutrons emitted from the moving fragments. It was assumed that, for a particular mass division, the scission neutrons were emitted from each fragment in the same proportions as those from the moving fragments. Thus ν, the total neutron emission from a particular fragment, is given by

$$\epsilon\nu = \frac{\epsilon\nu_F}{0.85} \qquad \ldots(5)$$

The data were normalised as before to $\bar{\nu}_p$ (Thermal) $^{235}U = 2.415$. It was unnecessary to repeat the process with the more accurate ν_T and scintillator efficiency data as subsequent corrections change the final data by less than 1 per cent. The details of the detector geometry and backscatter corrections are: if $P_i\ (M_i, E_T)$ are the observed experimental probabilities of neutron detection, then

$$P_1(M_1,E_T) = \nu_1\epsilon P_{11}(M_1,E_T) + \nu_2\epsilon P_{22}(M_2,E_T) \qquad \ldots(6)$$

and

$$P_2(M_2,E_T) = \nu_2\epsilon P_{21}(M_2,E_T) + \nu_1\epsilon P_{12}(M_1,E_T) \qquad \ldots(7)$$

where M_1 and M_2 are the complementary masses,

ν_1 and ν_2 are the neutron emission probabilities from complementary fragments,

ϵ is the liquid scintillator efficiency,

P_{i1} is the probability of forward neutron emission into the scintillator geometry of neutrons emitted from fragment i,

and P_{i2} is the probability of backward emission into the scintillator geometry of neutrons from fragment i.

The P_{i1} and P_{i2} probabilities were calculated as follows: it was assumed that the correlated neutrons were emitted isotropically in the centre of mass of the fragment and that the centre of mass neutron spectra were accurately represented by the usual evaporation spectra of temperature T, i.e.

$$\phi(E) \propto \frac{E}{T^2}\exp\left(-\frac{E}{T}\right) \qquad \ldots(8)$$

It was assumed that the temperature distribution for each fragment could be adequately represented by the experimentally determined mean centre of mass energy, $T = \frac{2}{3}\bar{E}$. The evaporation temperature data were taken from Kluge and Lajtai (1968). The laboratory probability distribution with respect to the fragment direction becomes

$$\rho_i(V_i,\theta) = \frac{a^2 v_i}{T_i^2}\ V_i^2\ \sin\theta\ \exp\left(-\frac{av_i^2}{T_i}\right) \qquad \ldots(9)$$

where V_i is the laboratory velocity of the neutrons

v_i is the neutron centre of mass velocity

$a = 0.5228$

θ is the neutron emission angle with respect to the fragment direction.

The laboratory velocity V_i is given by

$$V_i^2 = v_i^2 - W_i^2 + 2v_iW_i\cos\theta \qquad ...(10)$$

where W_i is the laboratory velocity of fragment i.

Since the scintillator subtends ± 24.5° the probabilities P_{il} and P_{i2} are given by

$$P_{il} = \int_0^\infty \int_0^{24.5^\circ} \rho_i(V_i,\theta)\, dV_i\, d\theta \qquad ...(11)$$

$$P_{i2} = \int_0^\infty \int_{155.5^\circ}^{\pi} \rho_i(V_i,\theta)\, dV_i\, d\theta \qquad ...(12)$$

These expressions were integrated numerically and equations 6 and 7 were solved to obtain $\epsilon\nu_i(M_i,E_T)$. For each fragment mass group, the neutron emission data were averaged over the kinetic energy distribution to obtain $\epsilon\nu_i(M_i)$. [The effect of the selected fragment distribution with respect to the axis of fragment detectors (± 8°) on the geometry factors P_{il} and P_{i2} was found to be relatively insignificant (< 1 per cent for A = 80 where geometrical corrections have their greatest effect)].

5. RESULTS AND DISCUSSION

5.1 Mass Distribution

The pre-neutron emission mass distribution, calculated as described from the raw kinetic energy data, is shown in Figure 3. The input (ν, E_T) data used in the correction procedure were taken from Maslin et al. (1967). In view of the close agreement of the present (ν, E_T) data with that of Maslin et al. it was unnecessary to recalculate the mass distribution using our (ν, E_T) data set.

The measured mass distribution is in good agreement with that obtained using more accurate methods such as radiochemical studies (Wahl 1965) and double velocity measurements using time of flight techniques (Milton and Fraser 1962). The fine structure observed in the mass distribution by Milton and Fraser (1962) is not strongly reproduced in the present data although both the light and heavy fragment distributions have shoulders. The magnitude of the fine structure actually observed is acceptable in view of the poorer mass resolution in double energy studies and the need for reasonable count rate.

The ratio of the asymmetric peak yield to the symmetric yield was approximately 110:1. This compares unfavourably with accepted values of 650:1 from radiochemical studies. In the symmetric region therefore only one in six events is genuine. Similar difficulties were experienced by Maslin et al. (1967) who obtained a ratio of 115:1.

5.2 Kinetic Energy Data

The mean total kinetic energy was found to be 170.8 MeV which is in good agreement with the value of 171.9 ± 1.4 from Schmitt et al. (1965) on whose work the correction procedure is based. The mean total kinetic energy as a function of the heavy fragment mass is plotted in Figure 4 together with similar data from Schmitt et al. (1966) and Maslin et al. (1967). Apart from the symmetric region, the present data are in good agreement with previous measurements. The measured dip in the kinetic energy curve at symmetric fission is 30 MeV which is slightly larger than recent estimates. Apalin et al. (1965) obtained a value of 21 MeV. Alexander et al. (1963) from measurements of fission fragment ranges placed the dip between 18 and 27 MeV. As in the data from Maslin et al. (1967) who measured a value of 33 MeV, the slightly larger dip at symmetric fission may be an effect of the anomalously large mass yield at symmetry.

5.3 Neutron Data

The measured variation of neutron emission with pre-neutron emission fragment mass averaged over the kinetic energy distribution and corrected as in Section 4 is shown in Figure 5. The errors shown in Figure 5 are purely statistical and are typically about 1.5 per cent at masses corresponding to the peaks in the mass distribution. Neutron data have not been plotted for the symmetric region where only one in six fission events is genuine. The curve in Figure 5 shows the usual trends observed in previous measurements. In particular the neutron yield near the spherical closed shell nuclei (N = 50, Z = 50) is very small and the yield from the easily deformed complementary fragments correspondingly high. The explanation of these features of the curve in terms of the deformability of the fragments is well known (Terrell 1962, 1965). The ratio of neutron yield from the light fragments to that from the heavy fragments $\frac{\nu_L}{\nu_H}$ was found to be 1.18. The exact magnitude of this value is very sensitive to the assumptions made in the correction procedure in Section 4.

The present data have been compared with those of Maslin et al. (1967) in Figure 6. The agreement between the two sets of data is particularly good. This of course should be expected as the experimental methods were similar. In Figure 7, a comparison is made with previous direct neutron counting data (Milton and Fraser 1965, Apalin 1965 and Maslin et al. 1967). Although the general features of all the data are similar, there are large discrepancies in the magnitude of the neutron emission. For the heavy fragments, the agreement is reasonably good although the large yield observed above A = 145 by Apalin et al. (1965) has not

been reproduced in any other data set. For the light fragments the agreement is very poor. Milton and Fraser (1965) and Apalin et al. (1965) both find the light fragment peak neutron emission to be significantly higher than either the present experiment or Maslin et al. (1967). For neutron emission at masses corresponding to the peak in the light fragment mass yield, the data of Milton and Fraser (1965) are significantly higher than the other three sets. Milton and Fraser (1965) have pointed out that backscatter corrections have not been made to their data and this correction has a significant effect on the neutron emission from the light fragment. For the very light fragments, $A < 90$, Apalin et al. (1965) measure a significantly smaller yield than do the other three experimenters. The cause of the discrepancies may be mass resolution in the cases of Maslin et al. and the present experiment or geometrical and backscatter correction in the other two cases. The poor peak to valley ratios obtained by Maslin et al. and in the present experiment suggest that there may be a mass resolution problem in these experiments. However in both experiments the peak to valley ratios are marred by the low energy tails in the single fragment spectra. These correspond to fragments which have been significantly degraded in energy for experimental reasons which are not clear. Their effect is to produce a background mass distribution beneath the genuine distribution. The influence of this background effect is of course far more significant for symmetric fission. If the analysis excludes fission events for which either fragment energy is in the tail region, a very significant improvement in the peak to valley ratio is obtained. Further, a careful examination of the mass-energy surface obtained in the present experiment with the corresponding data from Schmitt et al. (1966) shows very close agreement between the two sets of data for $E_T > 145$ MeV. These arguments suggest that the neutron versus fragment mass data in the present experiment are not significantly affected by poor mass resolution.

Milton and Fraser (1965) have reported fine structure in the neutron emission from the light fragment and, in particular, peaks in the neutron yield at masses 90, 96 and 101. This structure has not been observed in either of the other two previous measurements. There is a suggestion of structure in the present data which could with imagination be regarded as a mass resolution minimised version of the structure seen by Milton and Fraser (1965). Alternatively the data are statistically consistent with no structure.

Maslin et al. have observed a flattening of the neutron emission curve beyond mass 140 which is not apparent in the data of Apalin et al. (1965). Nor do the average data in Figure 5 show this flattening effect. However, if the present neutron data are plotted for different total kinetic energy ranges as in Figure 8, then the curves for the higher kinetic energy groups do show this flattening trend. The effect becomes more apparent with higher total kinetic energy. In this respect the present data are very similar to those of Maslin et al.

In Figure 9, the average neutron emission from both fragments averaged over the mass distribution is plotted as a function of the total kinetic energy. A least squares linear fit to the data in Figure 9 gives a value of - 0.167 MeV/neutron for the slope $\frac{dE_T}{d\nu}$. The comparable figure from Maslin et al. was - 0.185 MeV/neutron. The variation of neutron emission with fragment kinetic energy can be converted into the variation of neutron emission with fragment excitation (E^*) using the energy releases calculated from the Myers-Swiatecki (1966) mass formula. The value so obtained for $\frac{dE^*}{d\nu}$ was 9.5 MeV/neutron. Nifenecker et al. (1969) in their measurements of the variation of neutron emission with fragment charge and total kinetic energy obtained values between 9 and 10 MeV for $\frac{dE^*}{d\nu}$ for different Z. It is noteworthy that these values are significantly larger than the figure of 6.6 MeV generally regarded as necessary for the emission of a neutron. It has been suggested that the additional excitation is dissipated in gamma ray emission (Thomas and Grover 1967). Experiments have confirmed that the fission fragments are formed with high primary spins and since little angular momentum is carried off in neutron emission, the unavailability in daughter nuclei (formed by neutron emission) of high angular momentum states with relatively low excitation permits gamma ray competition. It is interesting to note that in a measurement of the variation of $\bar{\nu}_p$ with compound excitation in neutron fission of ^{235}U the slope of the $\bar{\nu}_p(E_n)$ curve below the pairing energy was found to be 0.107 neutron/MeV (Boldeman and Walsh 1970).

The variation in neutron emission per fragment with total kinetic energy for 8 selected mass groups 2 a.m.u. wide has been plotted in Figure 10. The variation for all 8 mass groups is linear. Similar curves are available for the other mass groups between A = 81 and A = 155 excepting the symmetric region but have not been reproduced here. However, Figure 11 is a plot of the least squares fitted slopes of the neutron emission versus total fragment kinetic energy curves as a function of the fragment mass.

6. ACKNOWLEDGEMENTS

The authors are indebted to the HIFAR Operations Staff for assistance during the course of these measurements, to Mr. H. Broe who played an important role in the design of the detector system and to the Instrumentation and Control Division who supplied some of the electronics and all of the surface barrier detectors.

7. REFERENCES

Alexander, J.M., Gazdik, M.F., Trips, A.R. and Wasif, S. (1963), Phys. Rev. 129, 2659.

Apalin, V.F., Gritsyuk, Yu.N., Kutikov, I.E., Lebedev, V.I. and Mikaelian, L.A. (1965), Nucl. Phys. 71, 546 and 553.

Boldeman, J.W., Lang, G.B., and Nicholson, K.P. (1962), AAEC/TM151.

Boldeman, J.W. and Dalton, A.W. (1967), AAEC/E172.

Boldeman, J.W. and Walsh, R.L. (1970), J. of Nucl. En. 24, 191.

Kluge, Gy. and Lajtai, A. (1968), Physics Letts. 27, 65.

Maslin, E.E., Rodgers, A.L. and Core, W.G.F. (1967), Phys. Rev. 164, 1520.

Milton, J.C.D. and Fraser, J.S. (1962), Can. J. of Phys. 40, 1626.

Milton, J.C.D. and Fraser, J.S. (1965), IAEA Symposium Physics and Chemistry of Fission Vol. 2, page 39.

Myers, W.D. and Swiatecki, W.J. (1966), Nucl. Phys. 81, 1.

Nifenecker, H., Frehaut, J. and Soleilhac, M. (1969), Second IAEA Symposium Physics and Chemistry of Fission, Vienna, page 491.

Schmitt, H.W., Gibson, W.M., Neiler, J.H., Walter, F.J. and Thomas, T.D. (1965), IAEA Symposium Physics and Chemistry of Fission, Vol. 1, page 531.

Terrell, J. (1962), Phys. Rev. 127, 880.

Terrell, J. (1965), IAEA Symposium Physics and Chemistry of Fission, Vol. 2, page 3.

Thomas, T.D. and Grover, J.R. (1967), Phys. Rev. 159, 980.

Wahl, A.C. (1965), IAEA Symposium Physics and Chemistry of Fission, Vol. 1, 317.

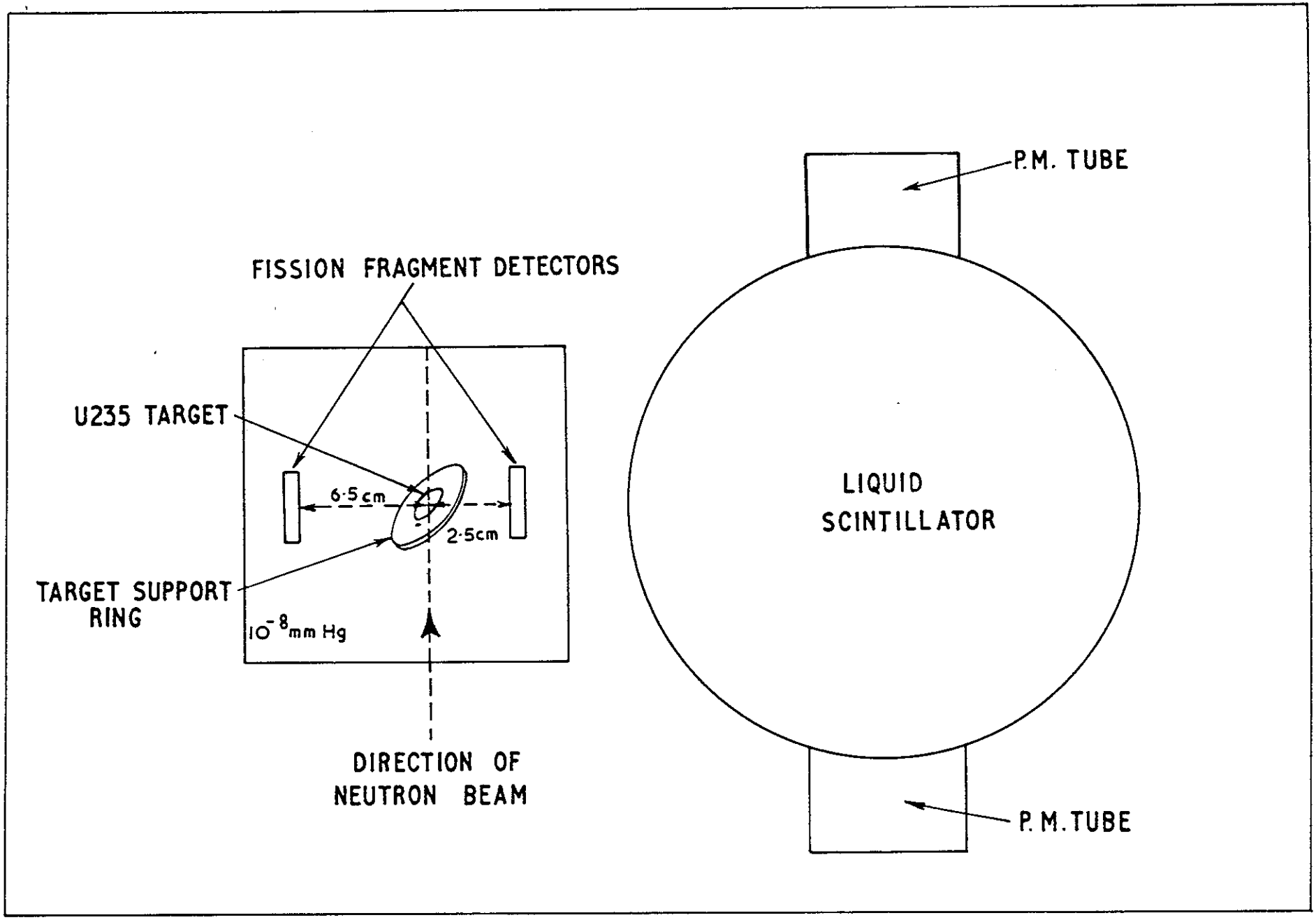

FIGURE 1. EXPERIMENTAL SYSTEM

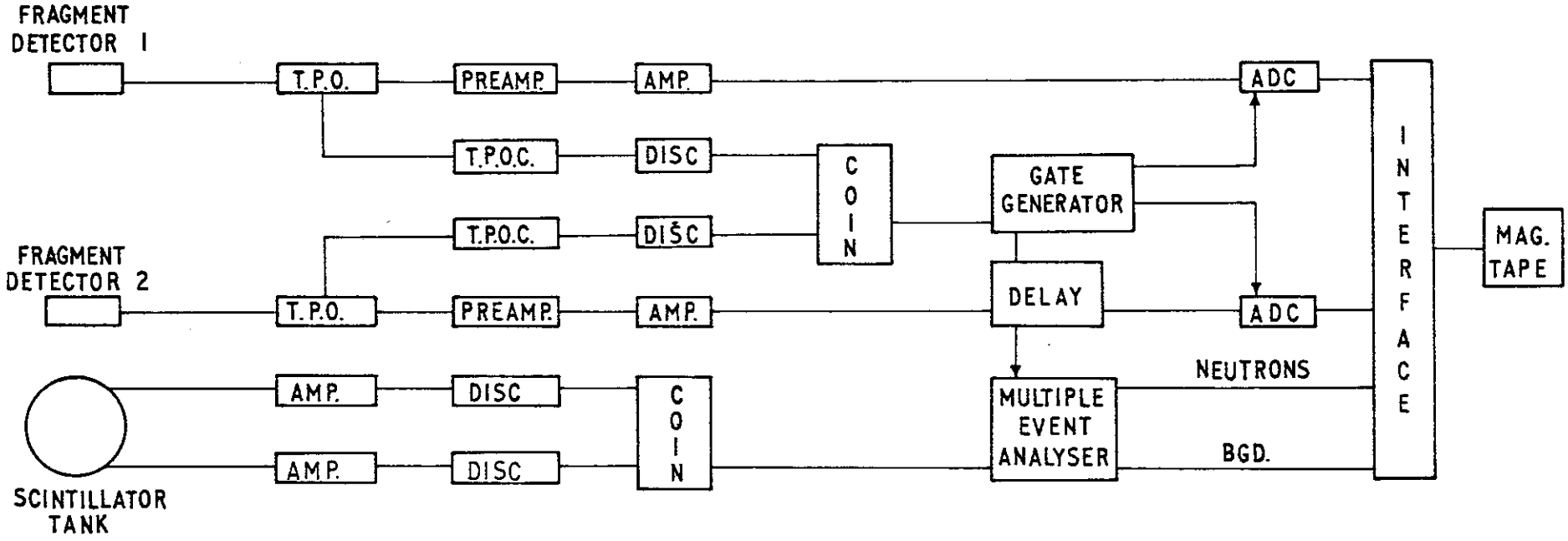

FIGURE 2. BLOCK DIAGRAM OF ELECTRONICS

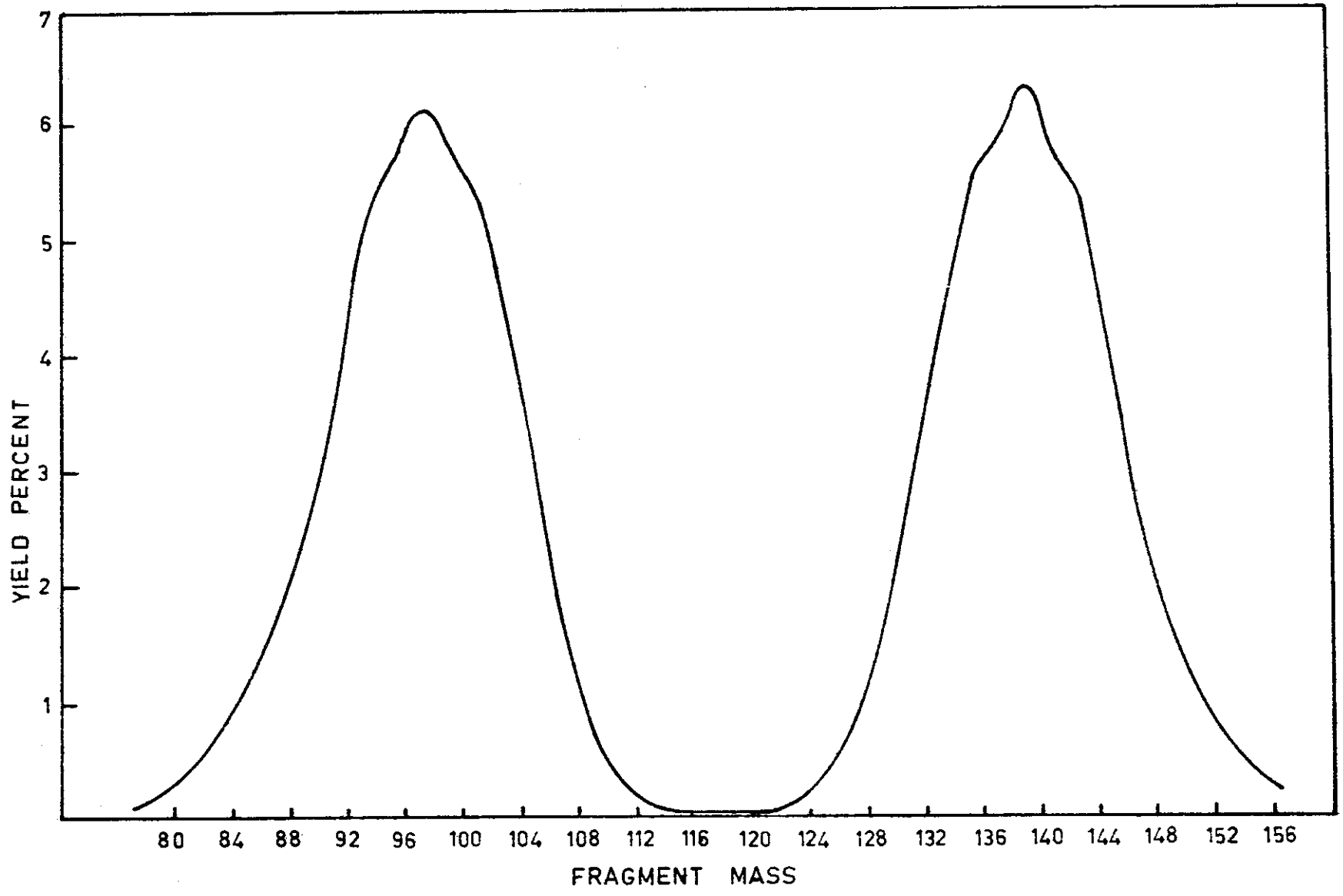

FIGURE 3. PRE-NEUTRON EMISSION MASS DISTRIBUTIONS

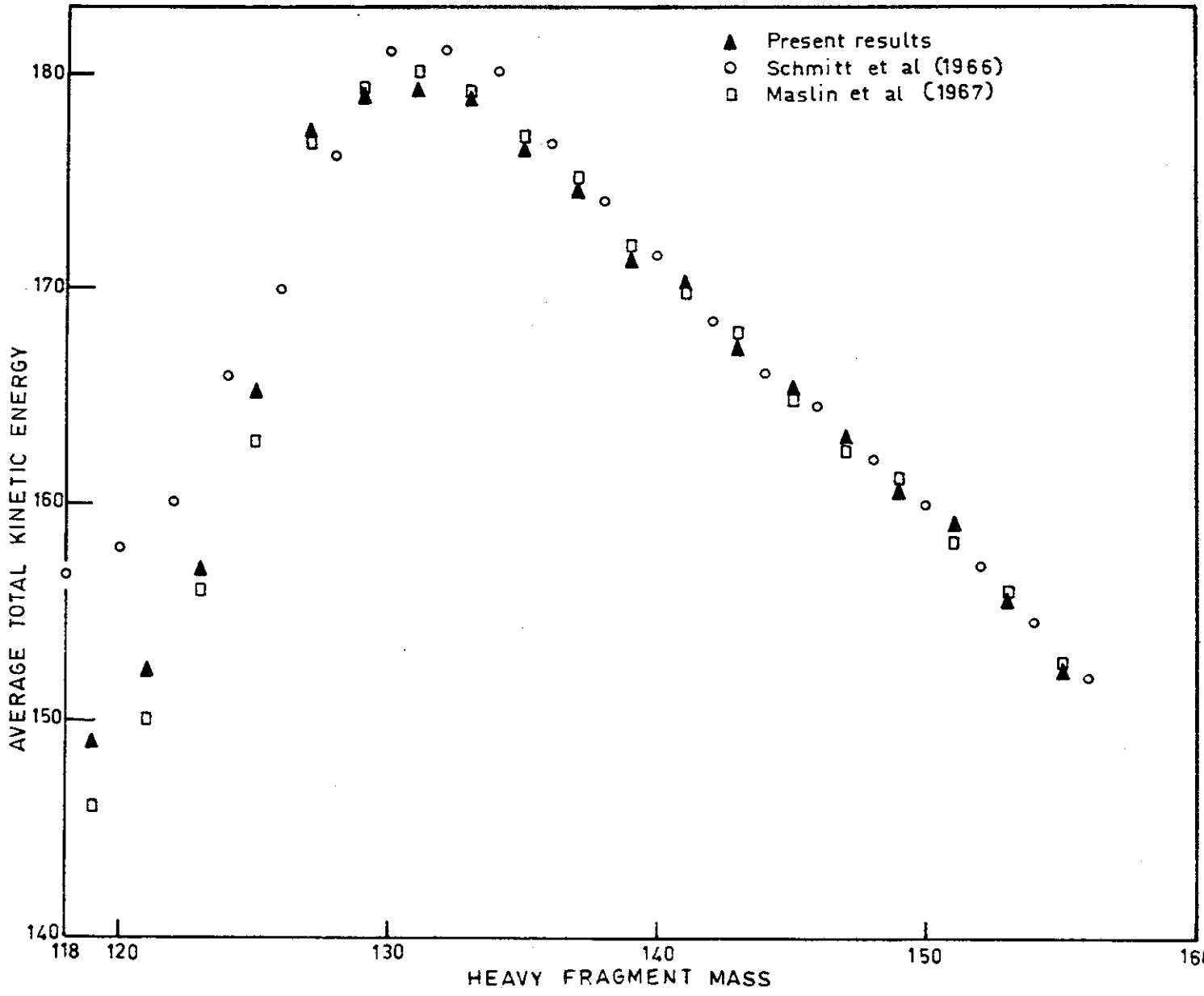

FIGURE 4. MEAN TOTAL FRAGMENT KINETIC ENERGY VERSUS HEAVY FRAGMENT MASS

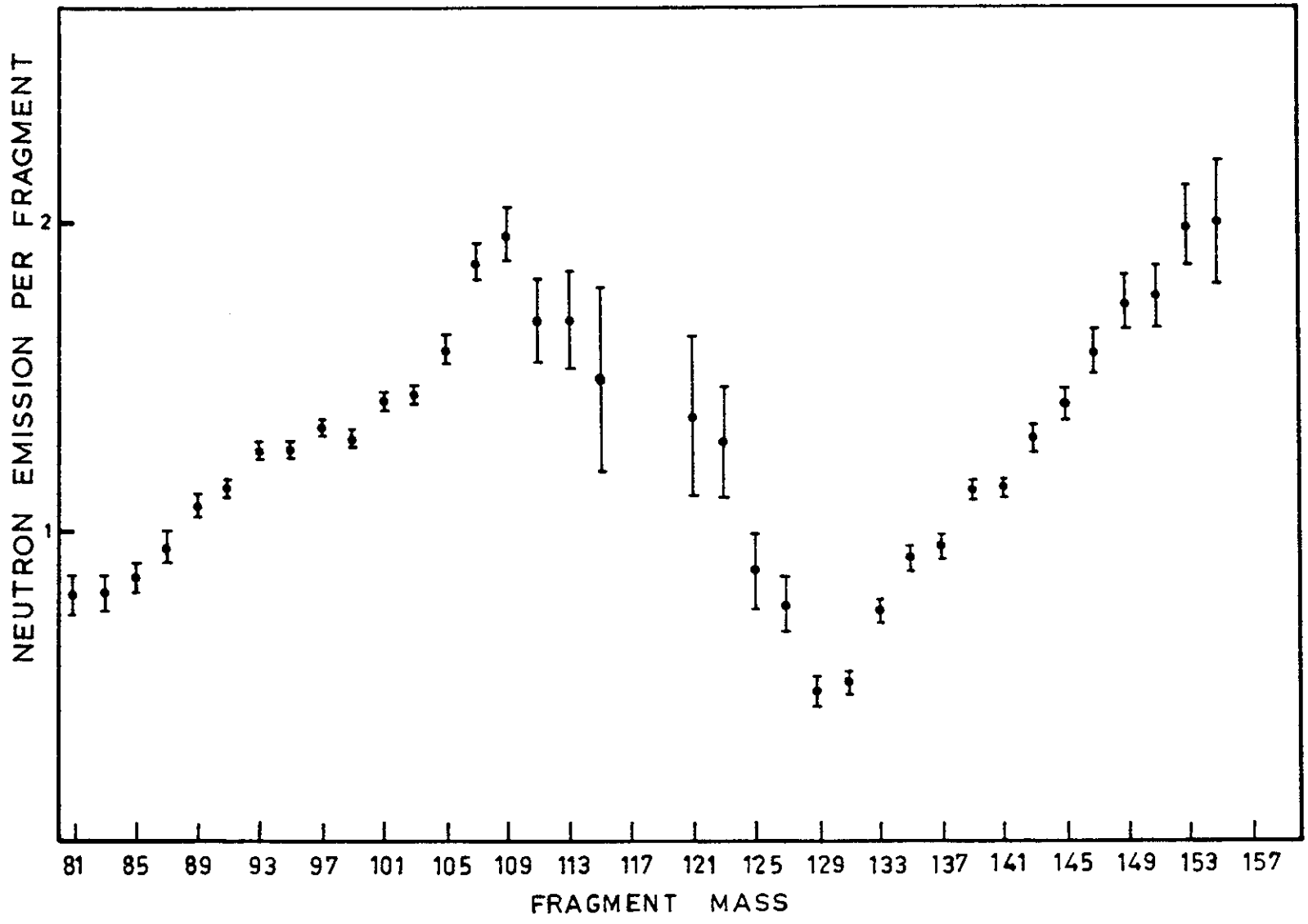

FIGURE 5. NEUTRON EMISSION PER FRAGMENT VERSUS FRAGMENT MASS

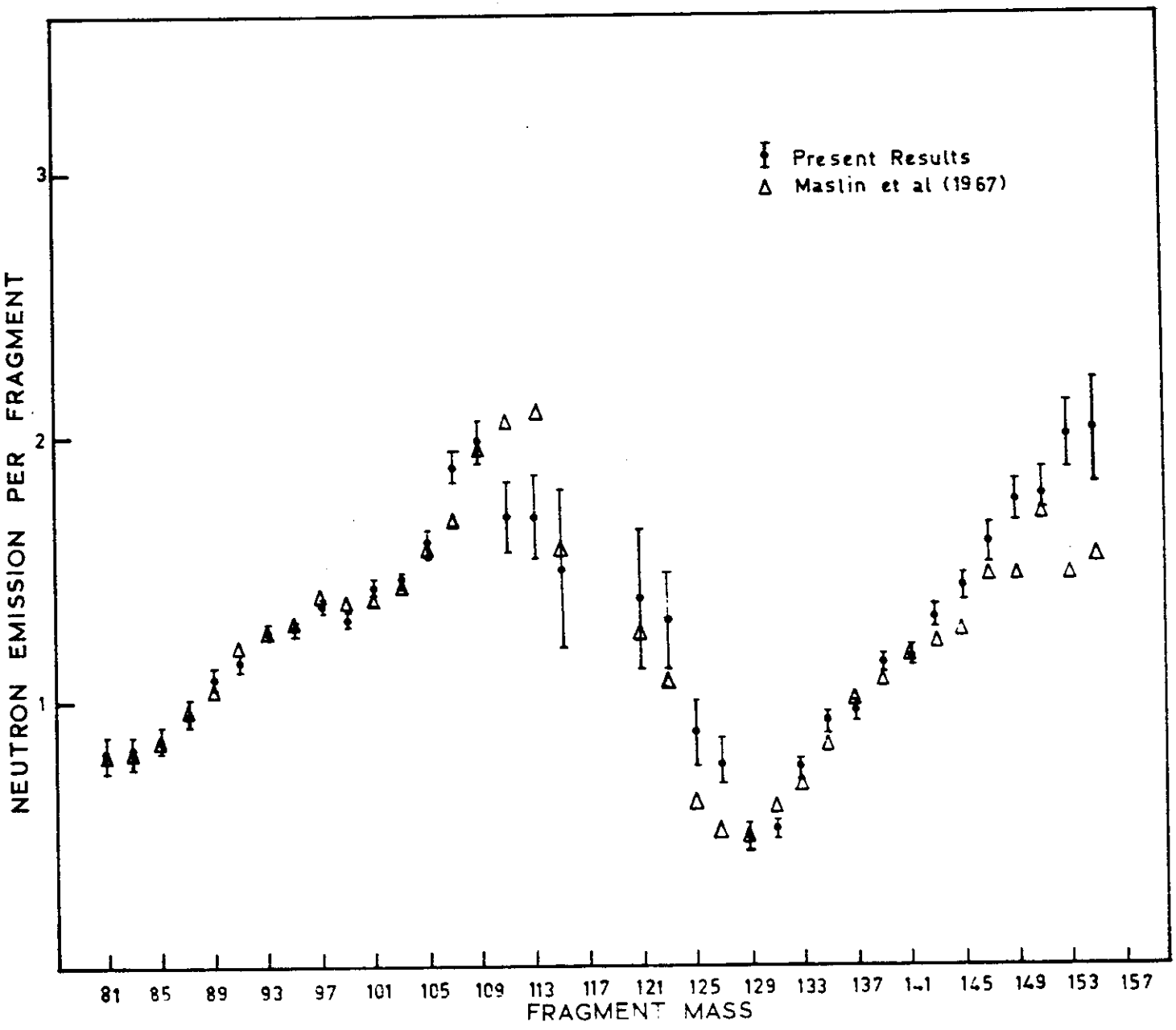

FIGURE 6. COMPARISON OF PRESENT DATA WITH THOSE OF MASLIN ET AL (1967)

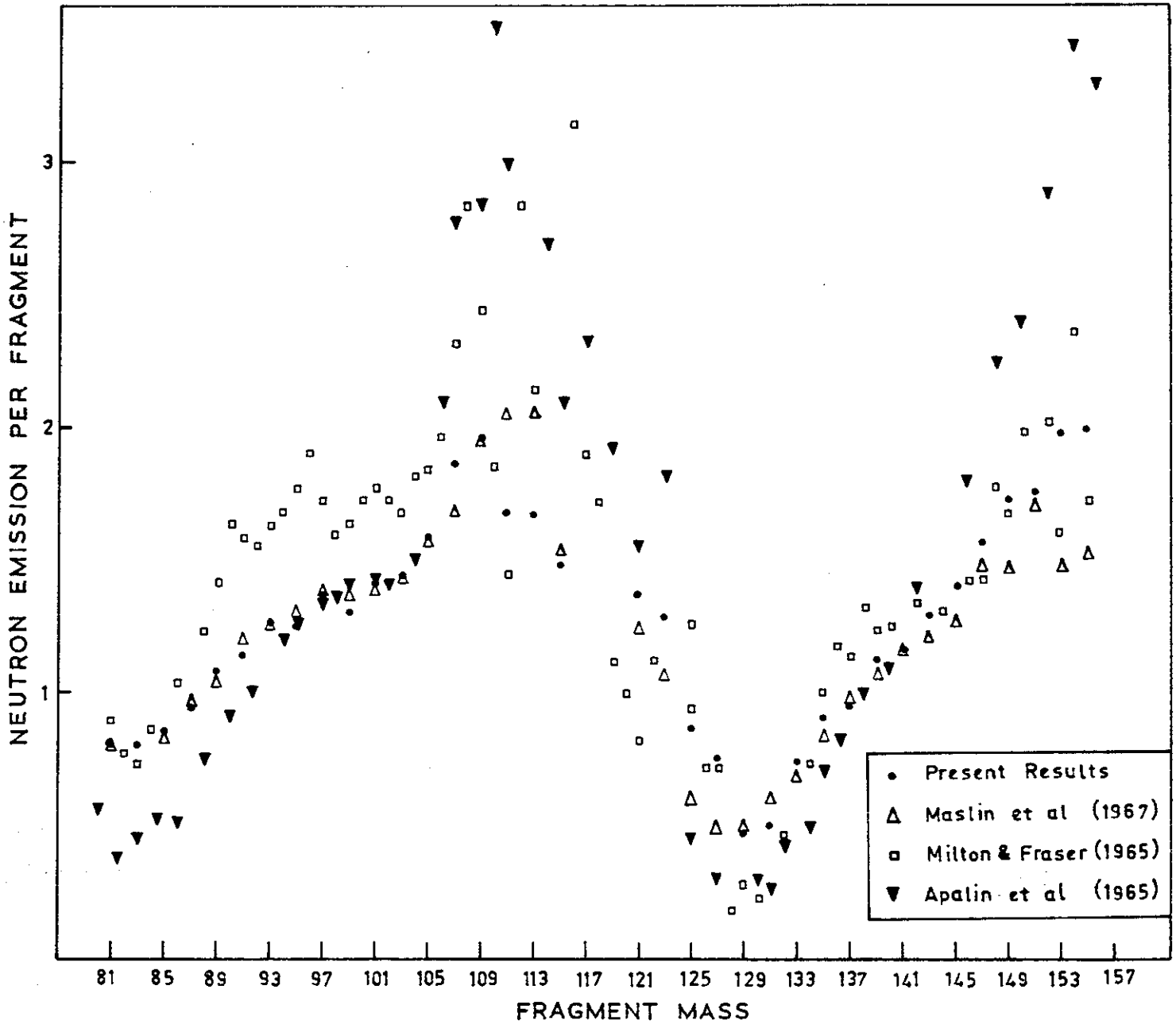

FIGURE 7. COMPARISON OF PRESENT NEUTRON EMISSION DATA WITH PREVIOUS DIRECT NEUTRON COUNTING DATA

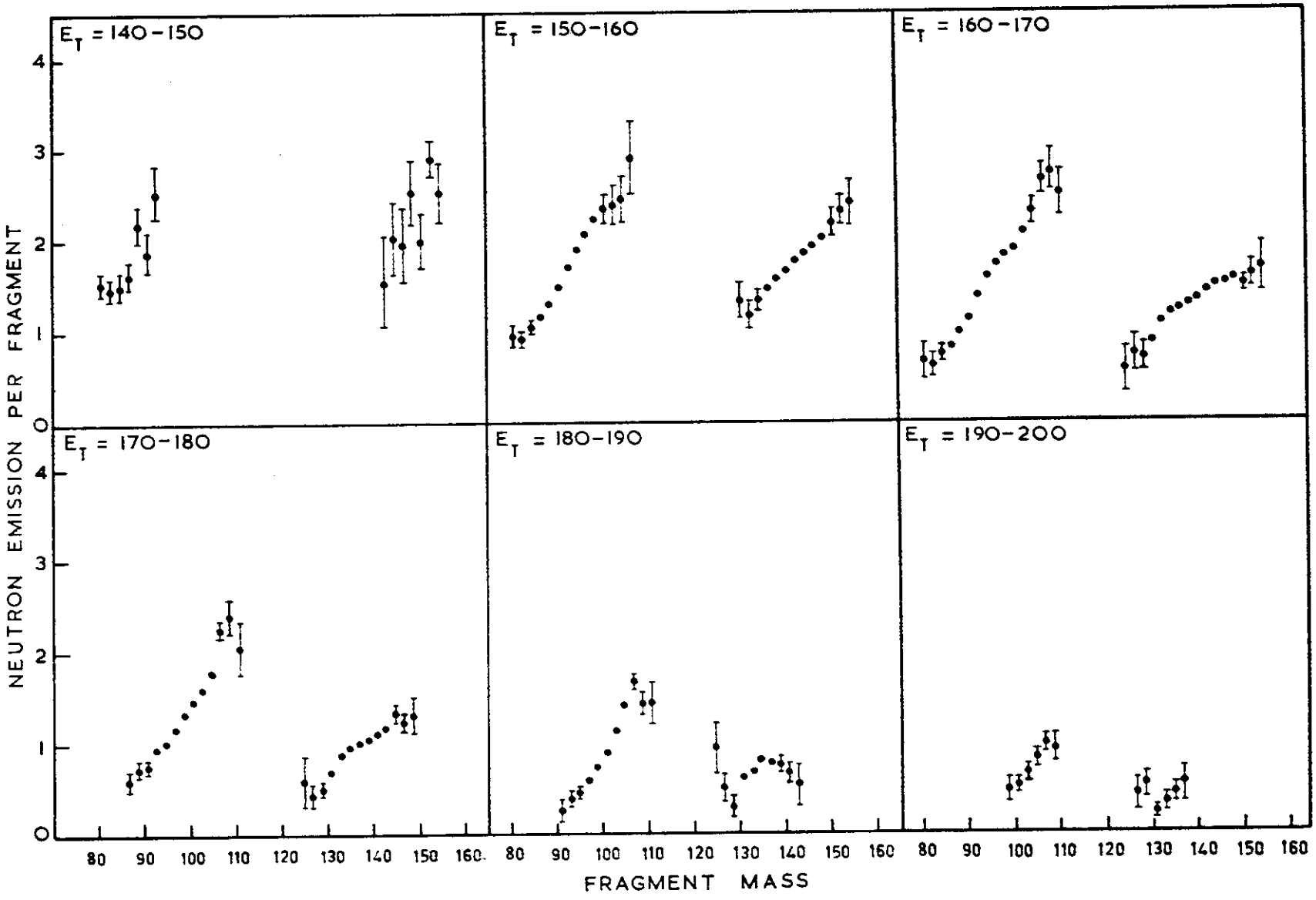

FIGURE 8. NEUTRON EMISSION PER FRAGMENT VERSUS FRAGMENT MASS FOR SIX RANGES OF TOTAL FRAGMENT KINETIC ENERGY

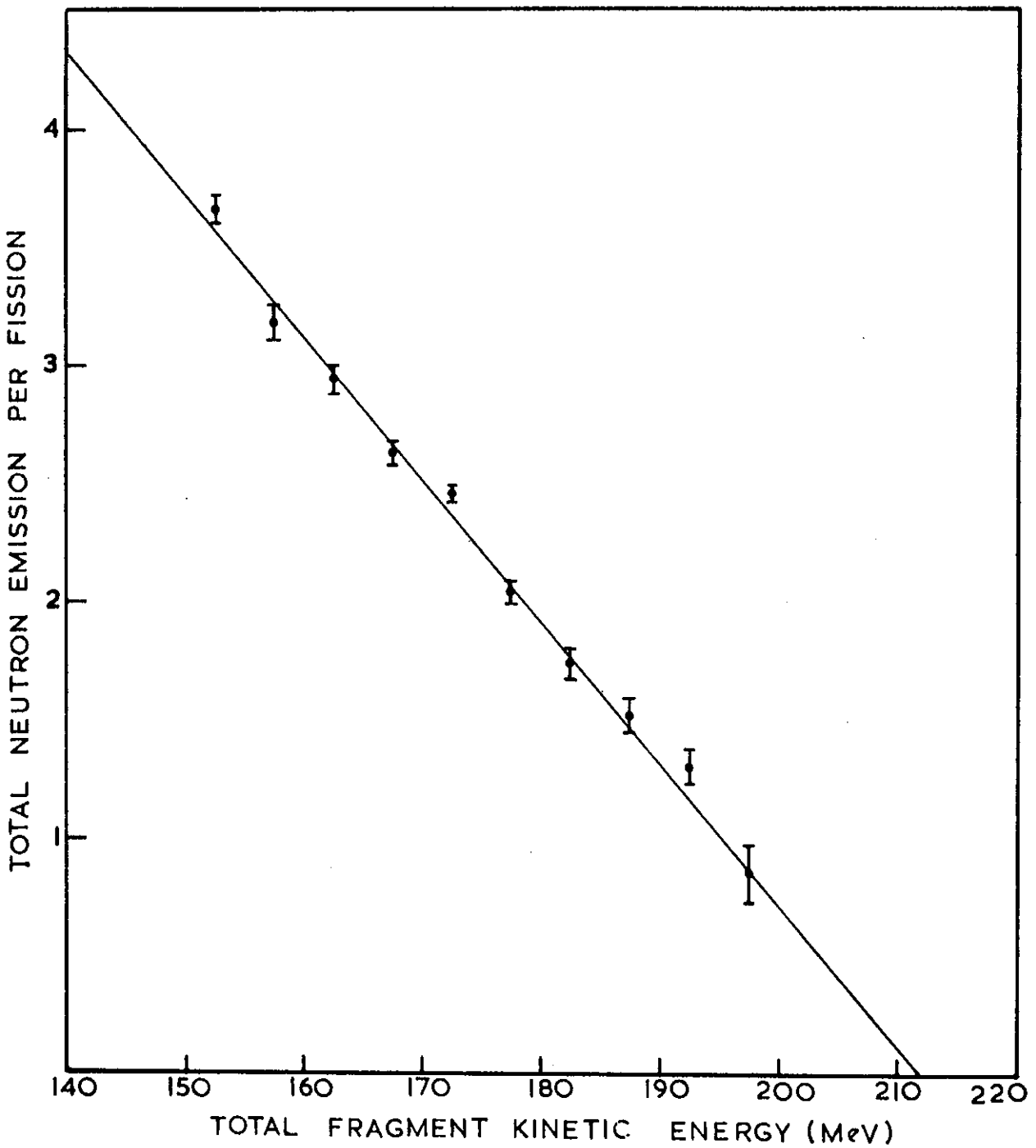

FIGURE 9. TOTAL NEUTRON EMISSION FROM BOTH FRAGMENTS PER FISSION VERSUS TOTAL FRAGMENT KINETIC ENERGY

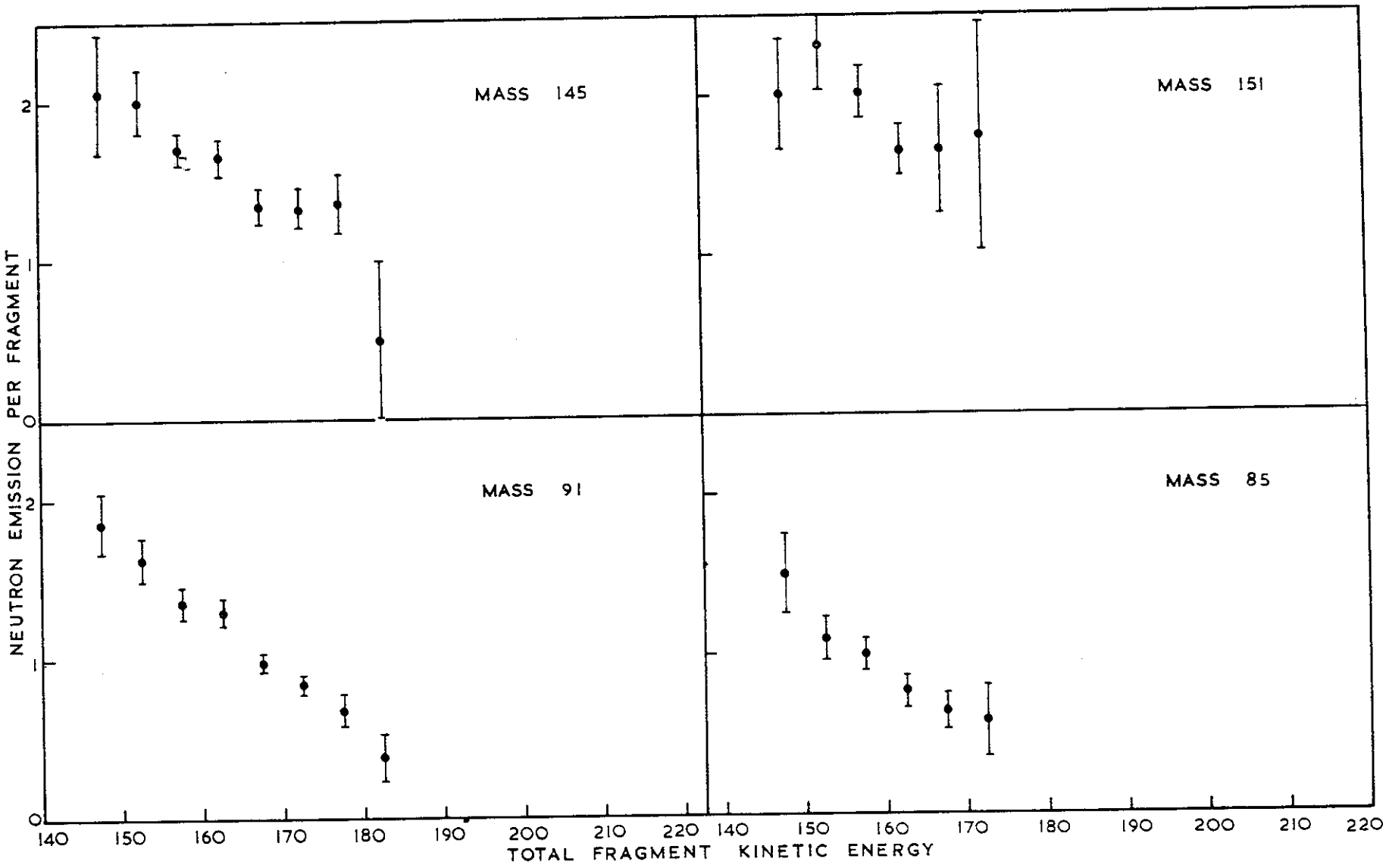

FIGURE 10a. NEUTRON EMISSION PER FRAGMENT VERSUS TOTAL FRAGMENT KINETIC ENERGY FOR EIGHT MASS GROUPS

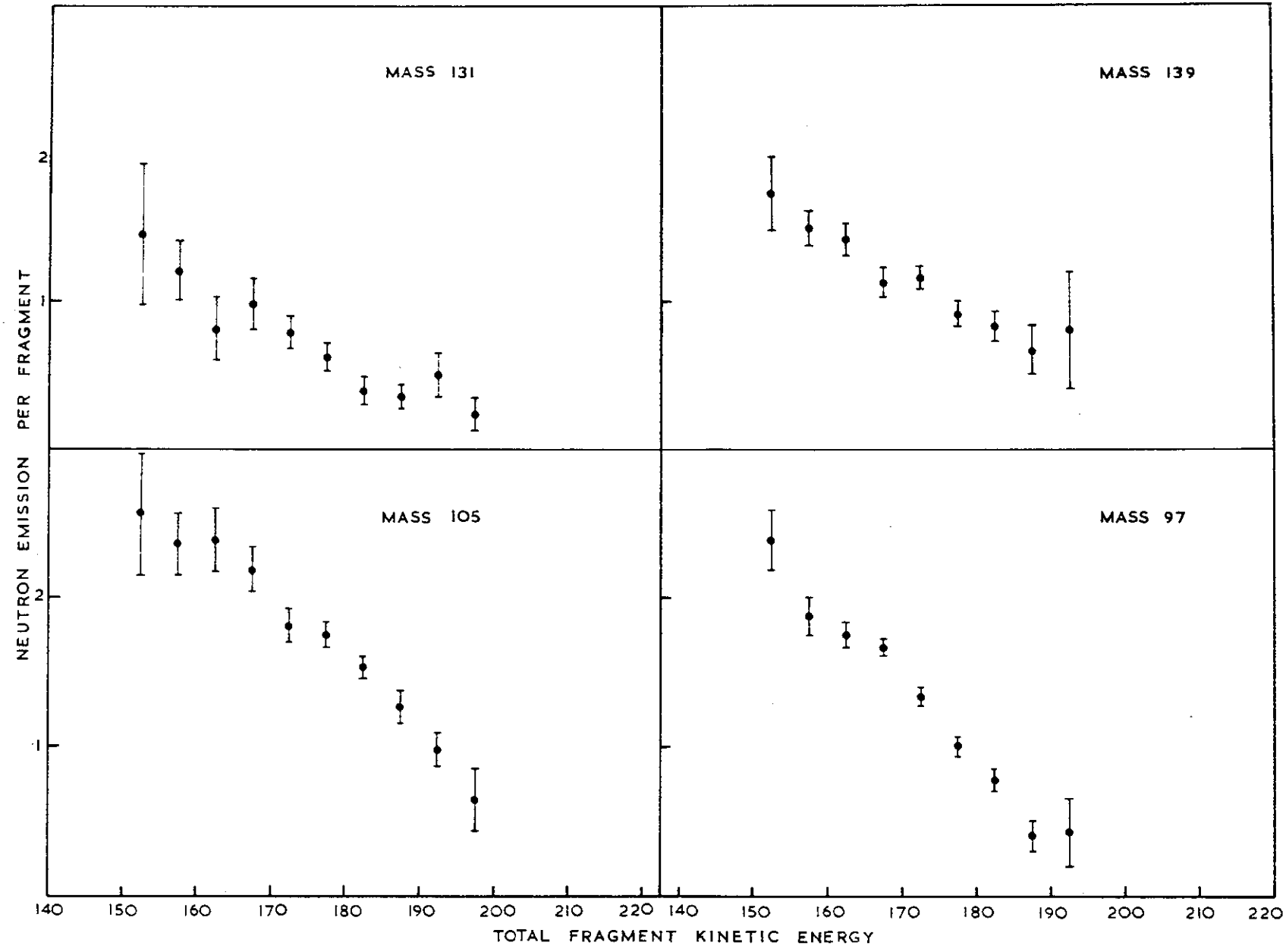

FIGURE 10b. NEUTRON EMISSION PER FRAGMENT VERSUS TOTAL FRAGMENT KINETIC ENERGY FOR EIGHT MASS GROUPS

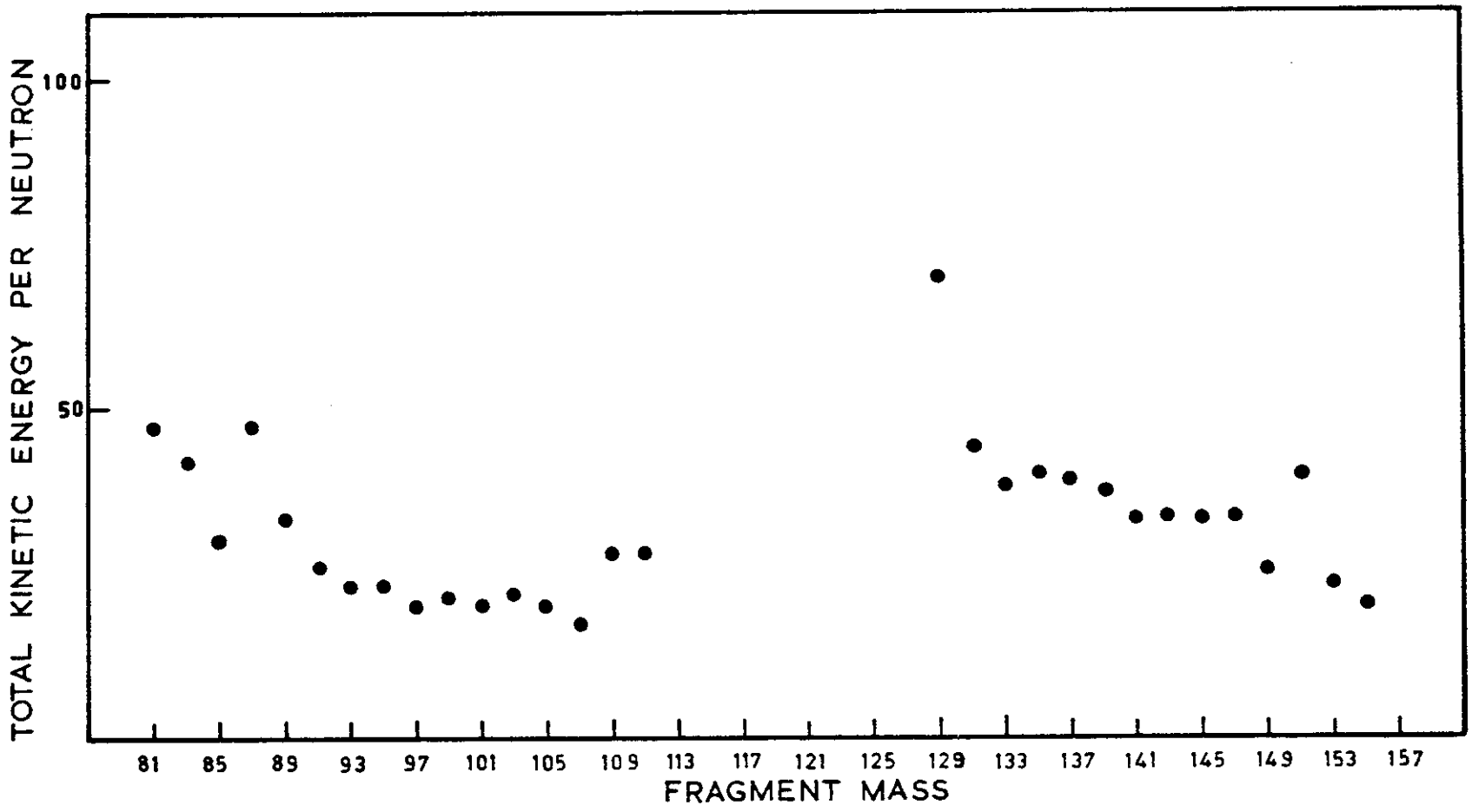

FIGURE 11. THE SLOPE $\frac{dE_T}{d\nu}$ VERSUS FRAGMENT MASS